MATEC Web of Conferences **180**, 02002 (2018) https://doi.org/10.1051/matecconf/201818002002
MET'2017

Application of supercapacitors in electric traction storage systems

Miroslaw Lewandowski[1,*], *Marek* Orzylowski[2], and *Maciej* Wieczorek[1]

[1] Warsaw University of Technology, Institute of Electrical Power Engineering, Electric Traction Division, ul. Koszykowa 75, 00-662, Warsaw, Poland
[2]University of Social Sciences, Information Technology Institute, ul. Sienkiewicza 9, 90-113, Łódź, Poland

Abstract. Energy storage systems (ESS) are based on electrochemical batteries and supercapacitors (SC). SCs have a lower energy density compared to batteries, but have an advantage over them in power density. The combined use of the two in a hybrid ESS (HESS) gives both high energy density and high power density of ESSs. Fractional-order impedance describes the SC dynamics better than commonly used integer order impedance. Such a description can be based on the dielectric relaxation equations e.g. Cole-Cole equation used in this work. The paper compares results of the impedance approximation of a number of SC's with various fractional and integer models, on the basis of which the time responses are analysed. The methods of capacitance and ESR measurement recommended by the IEC standard are examined. They are compared with the methods used in practice by SC producers. The problem of energy losses in ESS with respect to charging/discharging current pulses is presented. A proper ESS designing requires an accurate approximation of the SC impedance over the frequency band in which the dominant part of the power spectrum of current pulses is located.

1 Introduction

The braking energy of electric vehicles can be to a high degree retrieved and used again. In the case of traction vehicles, it can be transferred through a network to drive other vehicles. However, for full energy retrieval the energy storage systems (ESS) must be used. Numerous publications concern this topic, for example [1] or items listed in the bibliography of the work [2].

ESSs collect energy in electrochemical batteries and supercapacitors (SC), which have a lower energy density compared to that of batteries, but have an advantage over them regarding the power density. The combined use of the two makes it possible to achieve both high energy density and high power density of ESS. This is very important while receiving pulse energy during braking and giving it back during the acceleration of the vehicle.

When using SCs, it is necessary to take into account their specific dynamic properties resulting from the principle of their operation and construction. This article deals with this issue in relation to the ESS. It discusses the practical use of the descriptions of SCs dynamics, presented by different manufacturers and describes the problems of dynamic load of SC also.

2 Energy Storage Systems

Systems using both electrochemical and SC batteries are referred to as hybrid energy storage systems (HESS). An exemplary structure of the HESS system is shown in Fig. 1 [3]. Other HESS structures are described, for example, in [4].

ESS efficiency depends on losses in electrochemical batteries, SCs and DC/DC converters [5]. For example, [6] considers a stationary ESS that was located at the end of the tramline and was based solely on SCs (Fig. 2). It had the task of taking over and delivering energy up to 10 MJ (2.8kWh), necessary to speed up a tram. Losses in the inverters can be divided into the losses in chokes and those in the switching elements. In the system of Fig. 2, the copper and the core losses of the choke L are represented by the equivalent resistance R_L. The losses in transistors T_1 and T_2 and diodes D_1 and D_2 can be divided into conduction losses and switching losses. Analysis showed that the losses in these converter elements and those in the SC are comparable. It has also been estimated that total losses in SCs and DC/DC converters are generally lower than 10% of stored energy.

* Corresponding author: miroslaw.lewandowski@ee.pw.edu.pl

The mass and dimensions of the ESSs are affected by the used batteries, SCs and chokes. In the stationary ESS located at the end of a tram line [6] the value of stored energy required the use of SC battery made up of e.g. 20 pieces of 125 V Heavy Transportation Modules (Maxwell) with a unit capacitance of 63 F and a weight of 61 kg, i.e. of the total mass of more than 1200 kg.

In this case, the mass of the choke in the DC/DC converter depends on the voltage of used SC battery and in effect depends on the current charging/discharging the battery. It would be 100 kg - 200 kg depending on the parameters mentioned.

In this case, the mass of the choke in the DC/DC converter depends on the voltage of used SC battery and in effect depends on the current charging/discharging the battery. It would be 100 kg - 200 kg depending on the parameters mentioned. In the case of stationary ESS the weight does not much matter, although there is a problem of transmission losses. On the other hand, location of ESS on the vehicle increases the weight to be moved on and associated with it power consumption.

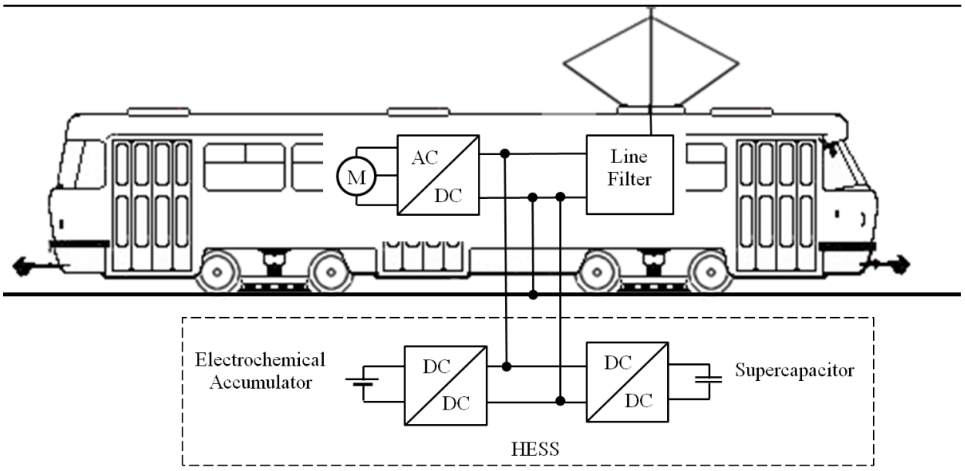

Fig. 1. Tramcar traction drive with hybrid energy storage system (parallel structure).

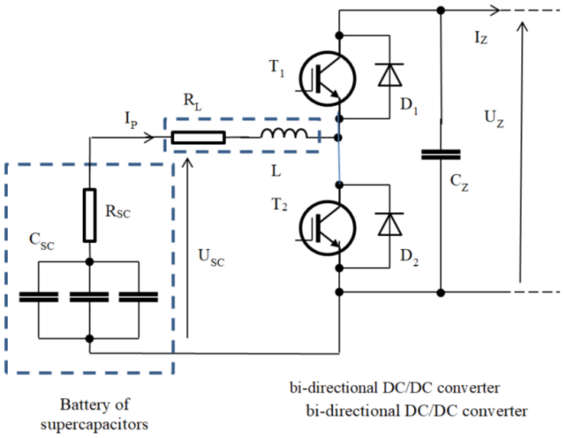

Fig. 2. Simplified scheme of ESS for the tram line, including SC battery and bi-directional DC/DC converter.

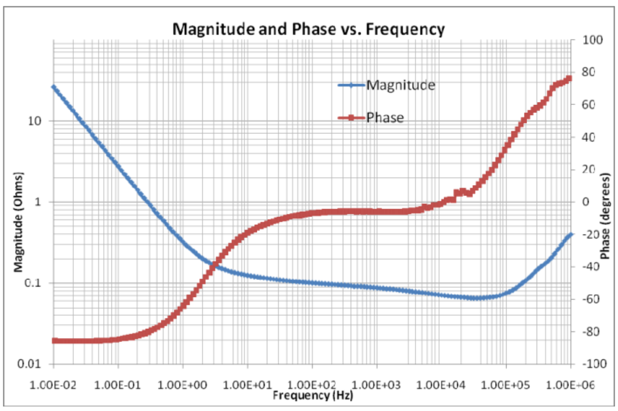

Fig. 3. Frequency response of HS206 (CAP-XX) of 0.6 F nominal capacitance.

3 Supercapacitor models and parameters

The specific properties of SCs result from the principle of their operation, which consists in the accumulation of electrical charge in the double electrical layer. This layer is formed by ions adsorbed on the surface of the porous electrodes. The very large surface of these electrodes allows for large capacities. An exemplary SC impedance graph over a wide frequency range is shown in Fig. 3. It follows from the plot that the capacitive nature of SC impedance exists in the range of lower frequencies. Above this range, the impedance of SC becomes resistive. The highest frequency range, in which the impedance is of inductive character, is of no significance for the matters considered here.

ESS designing, including the use of SC modules and energy flow control, requires the use of an accurate SC impedance model. Commonly used dynamics descriptions use transfer functions with integer exponents. The impedance of SC in this case has the general form

$$Z_I(s) = \frac{U(s)}{I(s)} = \frac{b_m s^m + b_{m-1} s^{m-1} \ldots b_1 s + b_0}{a_n s^n + a_{n-1} s^{n-1} + \cdots a_1 s + a_0} \qquad (1)$$

Reducing the number of coefficients of this model while increasing the accuracy can be achieved by replacing this description with a fractional description [7]. The fractional description in this case does not have a fully unambiguous physical interpretation, and the parameter values are determined experimentally. However, it should be taken into account that mathematical models only approximate some important features of systems and phenomena and serve for an effective solution to a given problem.

At the description by fractional differential equations, the SC impedance has the form

$$Z_F(s) = \frac{b_m s^{\beta m} + b_{m-1} m-1 + \cdots + b_1 s^{\beta_1} + b_0 s^{\beta_0}}{a_n s^{\propto n} + a_{n-1} s^{\propto n-1} + \cdots + a_1 s^{\beta_1} + a_0 s^{\propto_0}} \qquad (2)$$

where exponents αi and βi are real numbers. Description (2) may be based on the equations of dielectric relaxation in SC, such as the Cole-Cole equation of permittivity [8]

$$\varepsilon_{CC}(j\omega) = \varepsilon_\infty + \frac{\varepsilon_s - \varepsilon_\infty}{1+(j\omega T)^\delta} \quad 0 \leq \delta < 1. \qquad (3)$$

or that of the Cole-Davidson's [9].

$$\varepsilon_{CD}(j\omega) = \varepsilon_\infty + \frac{\varepsilon_s - \varepsilon_\infty}{(1+j\omega T)^\gamma} \quad 0 \leq \gamma < 1, \qquad (4)$$

The impedance description of ZCC(s), using the equation (3), is presented, for example, in [10]. The starting point for this was the equivalent circuit of a real capacitor in the form shown in Fig. 4.

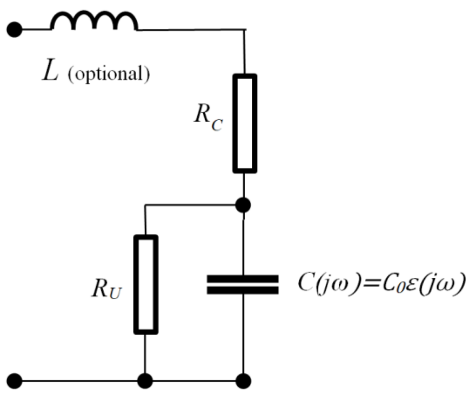

Fig. 4. An equivalent circuit of a supercapacitor.

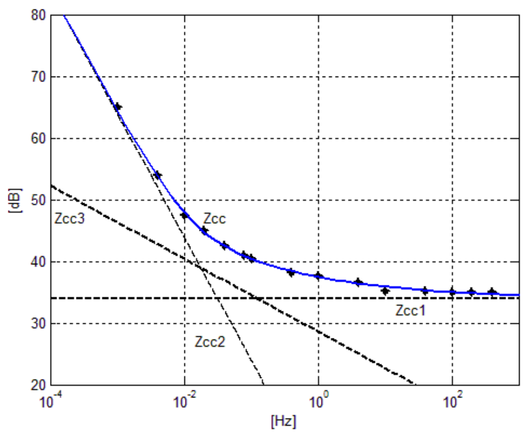

Fig. 5. Component moduli of impedances (6) of 0.1 F supercapacitor.

By omitting the inductance and after some simplification [12] this impedance can be presented as

$$Z_{cc}(s) = \frac{\left(1+\frac{R_c}{R_u}\right) + s^\delta \left(1+\frac{R_c}{R_u}\right) T^\delta + sR_cC}{\frac{1}{R_u} + sC} =$$

$$Z_{cc1}(s) + Z_{cc2}(s) + Z_{cc3}(s) \qquad (5)$$

where

$$Z_{cc1}(s) = R_c \qquad (6a)$$

$$Z_{cc2}(s) = \frac{R_u}{1+sR_uC} \qquad (6b)$$

$$Z_{cc3}(s) = \frac{s^\partial T^\partial R_u}{1+sR_uC} \qquad (6c)$$

To perform the frequency analysis, the Laplace transform should be replaced by its special case, which is the Fourier transform. This is done by substituting s = ω. The graph in Fig. 5 shows the approximation of the real frequency characteristic of the SC impedance by the fractional order model based on Cole-Cole equation. There are shown measured points marked by asterisks and the asymptotes connected with (6a)-(6c) SC impedance components.

The approximation of the real SC frequency response assumed by the authors was based on the minimization of the performance index of the form

$$J_f = \sqrt{\frac{1}{N-1} \sum_{i=1}^{N} \left(\frac{|Z_{CC}(j\omega_i) - Z_p(j\omega_i)|}{|Z_p(j\omega_i)|} \right)^2} \qquad (7)$$

where

- $Z_{CC}(j\omega)$ is the impedance approximating the real impedance of SC,
- $Z_P(j\omega)$ is the measured complex impedance of SC,
- ω_i is angular frequency for i^{th} measuring point.

This performance index can be treated as the standard deviation of the approximation error. The values of J_f performance indices for various SC models are collected in Table 1.

The SC impedance can be used to simulate the SC pulse responses, for example the voltage response to a square current wave excitation. The results of such simulations for a 2 Hz frequency, compared to real SC responses in the form of relative approximation errors, are also included in Table 1.

Table 1. Comparison of approximation accuracy of frequency and time responses of supercapacitors.

Capacity	Standard deviation of approximation by model							
	2nd order integer		3rd order integer		Cole-Cole		Cole-Davidson	
Response	freq.	time	freq.	time	freq.	time	freq.	time
0.047 F	9.8%	11.2%	5.3%	6.3%	5.1%	5.1%	3.5%	2.7%
0.1 F	10.5%	16.4%	4.4%	4.9%	4.8%	2.3%	3.8%	2.7%
0.33 F	16.3%	22.6%	7.8%	7.3%	7.8%	2.6%	5.4%	3.4%
0.6 F	13.7%	11.4%	10.0%	8.8%	10.4%	9.9%	14.0%	3.9%
100 F	8.0%	4.4%	5.8%	5.8%	6.2%	6.2%	6.0%	6.0%
2700 F	3.2%	2.4%	1.9%	2.2%	3.4%	5.4%	1.9%	3.1%

The results presented in Table 1 show that the Cole-Cole and Cole-Davidson models provide a similar level of approximation accuracy, with the Cole-Cole model being directly applicable to the standard impedance (2) determination. In addition, these models, with fewer coefficients, are more accurate than the 3rd order integer model.

A certain problem concerns the interpretation of the SC catalogue data of nominal capacity and nominal ESR. The reason is the suggested method of measurement.

IEC 62391-1: 2006 „Fixed electric double-layer capacitors for use in electronic equipment" standard [11] recommends the method that is based on the SC voltage waveform obtained during constant current discharging.

The methods for determining capacitance and internal resistance are illustrated in Fig. 6, as set forth in the description of the standard. In this drawing, the voltage vs. time graph is approximated by straight lines.

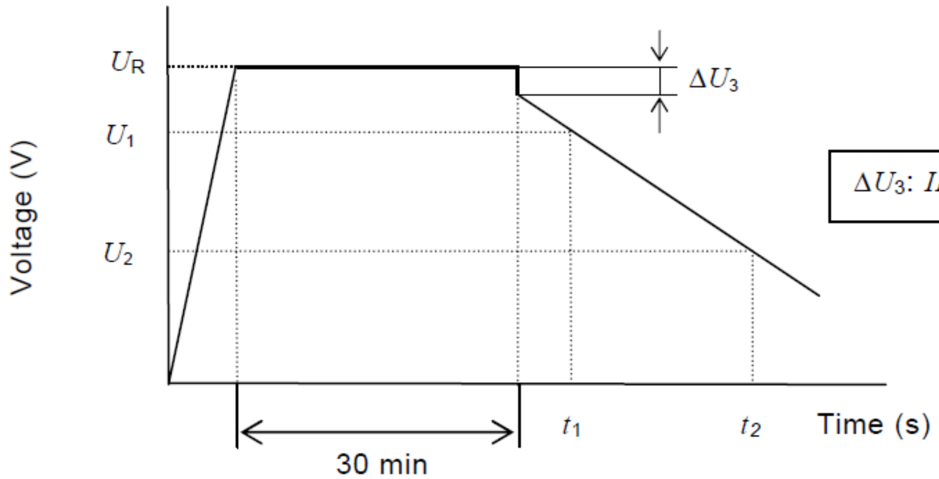

Fig. 6. Voltage on the capacitor terminals during the capacitance and ESR measurements according to IEC 62391-1: 2006 standard [11].

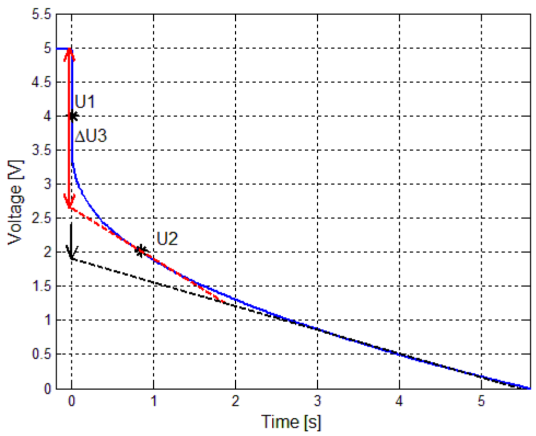

Fig. 7. The discharge of the supercapacitor of 1 F nominal capacitance with 200 mA current according to IEC Standard for Class 4. Measurement results: C=0.08 F, R=14 Ω.

The measurement takes place during constant current discharge I. The capacity is determined by the dependence

$$C = \frac{I \times (t_2 - t_1)}{U_1 - U_2} \quad (8)$$

while the internal resistance by the dependence

$$R = \frac{\Delta U_3}{I} \quad (9)$$

As mentioned, the standard assumes that the SC voltage response to a step current excitation can be well approximated by straight lines. Meanwhile, the component (6c) of impedance (5) can cause a significant nonlinearity of this response. This is illustrated in Fig. 7, showing such a response for one of SC types of 1 F capacitance. The response concerns the discharge current recommended for the class 4 standard described as "instantaneous power". This class corresponds to a pulse mode work of SC in ESS. The voltage levels and the linear approximation are marked on this graph, which are taken into account in (8) and (9). Direct application of this kind of result leads, among other things, to the determination of the capacitance by the order of magnitude lower than nominal. The standard allows to change the value of discharge current, but it makes it very imprecise.

As a result of the occurrence of such cases, producers do not fully apply IEC 62391-1: 2006 standard or do not use it at all. In addition, they supplement the technical data of the measurements according to their own methods. Table 2 shows, for example, the measurement methods of three SC module manufacturers that can be used to build ESS [Lewandowski et al. (2016)]. Because of these differences when designing SC systems, it is necessary to know the individual methods of measuring their parameters.

Table 2. Methods of determination of capacitance and ESR.

Producer	Method of capacitance measurement	Methods of ESR measurement	
Ioxus	IEC method, discharge current specified for Class 3	DC method: Discharge current specified for IEC Class 4	ΔU_3 drop (IEC method)
			Voltage drop after 10 ms
		AC method: Resistance for 1 kHz	
Skeleton	Method similar to IEC method, current specified for Class 3	DC method: Discharge current specified for IEC Class 3	ΔU_3 drop (IEC method)
			Voltage drop after 10 ms
		AC method: Resistance for 100 Hz	
Maxwell	Own method with sequence of current steps	Own method with sequence of current steps	

4 Energy losses under dynamic conditions

The analysis presented in [6] treats the processes of loading and unloading the SC battery in ESS in a static manner, that is, it does not take into account the duration of these processes and the transient states associated with them. This approach is sufficient to estimate the level of losses in individual ESS blocks. However, for the design of ESS it is desirable to analyze the dynamic conditions typical for the operation of these systems.

The graph in Fig. 3 shows that for lower frequencies the SC impedance is capacitive, while for higher - resistive. The boundary between the two usually corresponds to the time constant of dielectric relaxation and lies generally in the range of 0.01÷10 Hz. The value of those limits are important because of the frequency spectrum of the current pulses during braking and acceleration of the vehicle.

The pulse of unitary amplitude and the duration of $-T_0/2<t<T_0/2$ has the Fourier transform of the form

$$I_p(j\omega) = sinc\left(\frac{\omega T_0}{2}\right) \qquad (10)$$

Let us consider a couple of pulses of the current $i_{pp}(t)$ charging and discharging SC that are shown in Fig. 8. These pulses have unitary amplitudes, the duration of T_0, and are shifted from the centre of the coordinate system by $\pm\tau$. The Fourier transform of the signal i_{pp}(t) has the following form

$$I_{pp}(j\omega) = sinc\left(\frac{\omega T_0}{2}\right) e^{j\omega\tau} - sinc\left(\frac{\omega T_0}{2}\right) e^{-j\omega\tau} \qquad (11)$$

Using Euler formula it can be written as

$$I_{pp}(j\omega) = sinc\left(\frac{\omega T_0}{2}\right) [e^{j\omega\tau} - e^{-j\omega\tau}\,] =$$

$$= -2j sinc\left(\frac{\omega T_0}{2}\right) sin(\omega\tau) \qquad (12)$$

The energy spectrum of the signal i_p (t) depends on length T_0 of the braking and acceleration current pulses. Significant influence on this spectrum has also the time shift τ of these pulses. Let us consider the cases of different lags, shown in Fig. 9. Exemplary energy spectra normalized to pulse length T_0 are shown in Fig. 10.

It follows from Fig. 10 that the dominant parts of the power spectra of the pulses under consideration are located below the frequency

$$f_0 = \frac{1}{T_0} \qquad (13)$$

Considering the energy loss analysis during storage in SC, it is important to take into account the frequency characteristic of SC in the range of the significant part of the current pulse spectrum. The analysis shows that shortening these pulses during braking or acceleration reduces the energy efficiency of ESS. This analysis will be presented in one of the following papers.

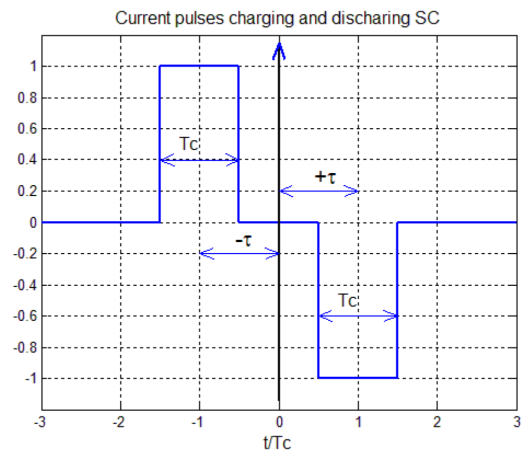

Fig.8. Graph of the normalized current charging and discharging SC.

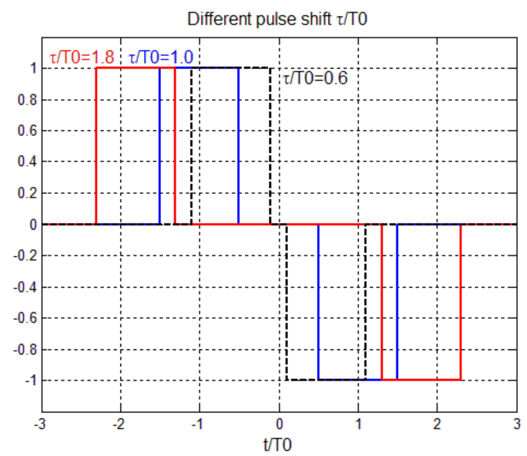

Fig. 9. Pulses of charging and discharging current shifted in time.

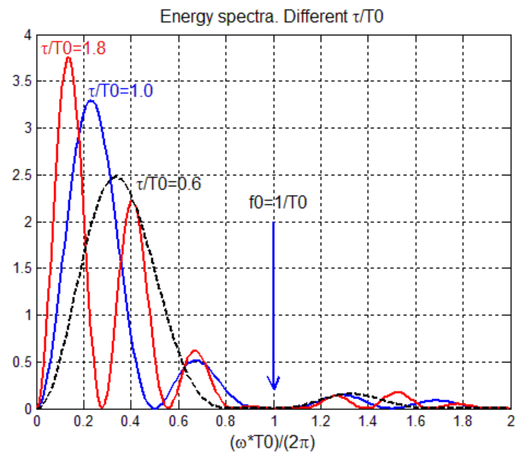

Fig. 10. Energy spectra of pulses shown in Fig. 9.

5 Conclusions

For proper electric vehicle ESS designing, the accurate SC model must be used. Such the model is the fractional order model. Among others this model allows one to analyze the measurement problems of SC parameters. It also allows one to analyze the influence of the dynamics of braking and acceleration of the electric vehicle on the energy efficiency of the ESS.

References

1. A. Szeląg, *The influence of the voltage in the 3kV DC traction network on the energy and traction parameters of supplied vehicles* (INW SPATIUM, 2013) ISBN: 978-83-62805-01-3 [in Polish]
2. M. Wieczorek, and M. Lewandowski, *A mathematical representation of an energy management strategy for hybrid energy storage system in electric vehicle and real time optimization using a genetic algorithm*, Applied Energy, **192**, 222–233 (2017) doi: 10.1016/j.apenergy.2017.02.022
3. G. Zaleskis, V. Brazis, and L. Latkovskis, *Estimation of Traction Drive Test Bench with Energy Storage System Operation in Regenerative Braking Mode*, Electrical, Control and Communication Engineering, **1**, 40-45 (2012) doi: 10.2478/v10314-012-0007-y
4. Ziyou Song, Heath Hofmann, Jianqiu Li, Xuebing Han, Xiaowu Zhang, and Minggao Ouyang, *A comparison study of different semi-active hybrid energy storage system topologies for electric vehicles*, Journal of Power Sources, **274**, 400-411 (2015) doi: 10.1016/j.jpowsour.2014.10.061en
5. J. Leuchter, P. Bauer, P. Bojda, and V. Rerucha, Bi-Directional DC-DC Converters for Supercapacitor Based Energy Buffer for Electrical Gen-Sets, *European Conference on Power Electronics and Applications, Aalborg* (2-5 Sept., 2007) ISBN 9789075815108
6. M. Lewandowski, M. Orzylowski, and A. Buze, *Power losses in energy storage system for* tram line, Przegląd Elektrotechniczny, **R.92**, Nr 12/2016, 289-295 (2016) doi:10.15199/48.2016.12.71 [in Polish]
7. C. A. Monje, Y. Chen, B. M. Vinagre, D. Xue, V. Feliu-Batlle, *Fractional-Order Systems and Controls: Fundamentals and Applications* (Springer, 2010) doi: 10.1007/978-1-84996-335-0
8. J-L. Déjardin, and J. Jadzyn, *Determination of the nonlinear dielectric increment in the Cole-Davidson model*, The Journal of Chemical Physics, **125**, 114503, (2006), doi: 10.1063/1.2346378
9. A. Dzieliński, G. Sarwas, and D. Sierociuk, *Comparison and Validation of Integer and Fractional Order Ultracapacitor Models*, Advances in Difference Equations, (Springer, 2011) doi:10.1186/1687-1847-2011-11
10. M. Lewandowski, and M. Orzyłowski, *Fractional-Order Models: The Case Study of the Supercapacitor Capacitance Measurement*, Bulletin of the Polish Academy of Sciences: Technical Sciences, **65**(4), 449-457 (2017) doi: 10.1515/bpasts-2017-0050
11. International Standard IEC 62391-1:2006, *Fixed electric double-layer capacitors for use in electronic equipment*, Part 1: Generic Application, IEC (2006)
12. M. Orzylowski, and M. Lewandowski, *Computer Modeling of Supercapacitor with Cole-Cole Relaxation Model*, Journal of Applied Computer Science Methods, **2**(4), 105-121 (2013) ISSN 1689-9636